Electronic Supplementary Material (ESI) for Analytical Methods.


# Electronic Supplementary Information

# Direct detection of tryptophan for rapid diagnosis of cancer cells metastasis competence by ultra-sensitive and highly selective electrochemical biosensor

M. R. Majidi,[a*] P. Karami,[a,b] M. Johari-Ahar,[b] and Y. Omidi[b*]

[a.] Department of Analytical Chemistry, Faculty of Chemistry, University of Tabriz, Tabriz, Iran. Email: majidi@tabrizu.ac.ir; fax: +98 41 33340191; Tel: +98 41 33393111

[b.] Research Center for Pharmaceutical Nanotechnology, Faculty of Pharmacy, Tabriz University of Medical Sciences, Tabriz, Iran. Email: yomidi@tbzmed.ac.ir; Fax: +98 41 33367929; Tel: +98 41 33367914

**Characterization of the prepared electrodes**

**Determination of active surface area of the modified electrodes**

To assess whether modification of electrode with MWCNT and Apt molecules can affect the effective surface area of the modified electrodes, we determined the effective working area of the bare AuE, MWCNT-AuE, and Apt-MWCNT-AuE using linear sweep voltammetry (LSV) based on Randles-Sevcik relationship[1]. Equation (Eq.) S1 was employed to determine the reduction of redox couple of $K_3[Fe(CN)_6]$ and $K_4[Fe(CN)_6]$ (1.0 $_m$M ) in DI-water containing potassium chloride (0.1 M).

Eq. S1:

$$i_p = 0.446\, nFAC \left(\frac{nF}{RT}\right)^{1/2} \upsilon^{1/2}\, D^{1/2} = \left(2.96 \times 10^5\right) n^{3/2} A D^{1/2} \upsilon^{1/2} C \; [25^{\circ}C]$$

Where, $i_p$ represents the peak current (A), n (=1) refers to the number of electrons transferred, A is the effective area of the electrode ($cm^2$), D is the diffusion coefficient of $[Fe(CN)_6]^{3-}$ (taken to be $7.60\times10^{-6}$ $cm^2.s^{-1}$), C represents the concentration ($mol.cm^{-3}$), υ is the scan rate ($V.s^{-1}$), and other symbols have their usual meaning.

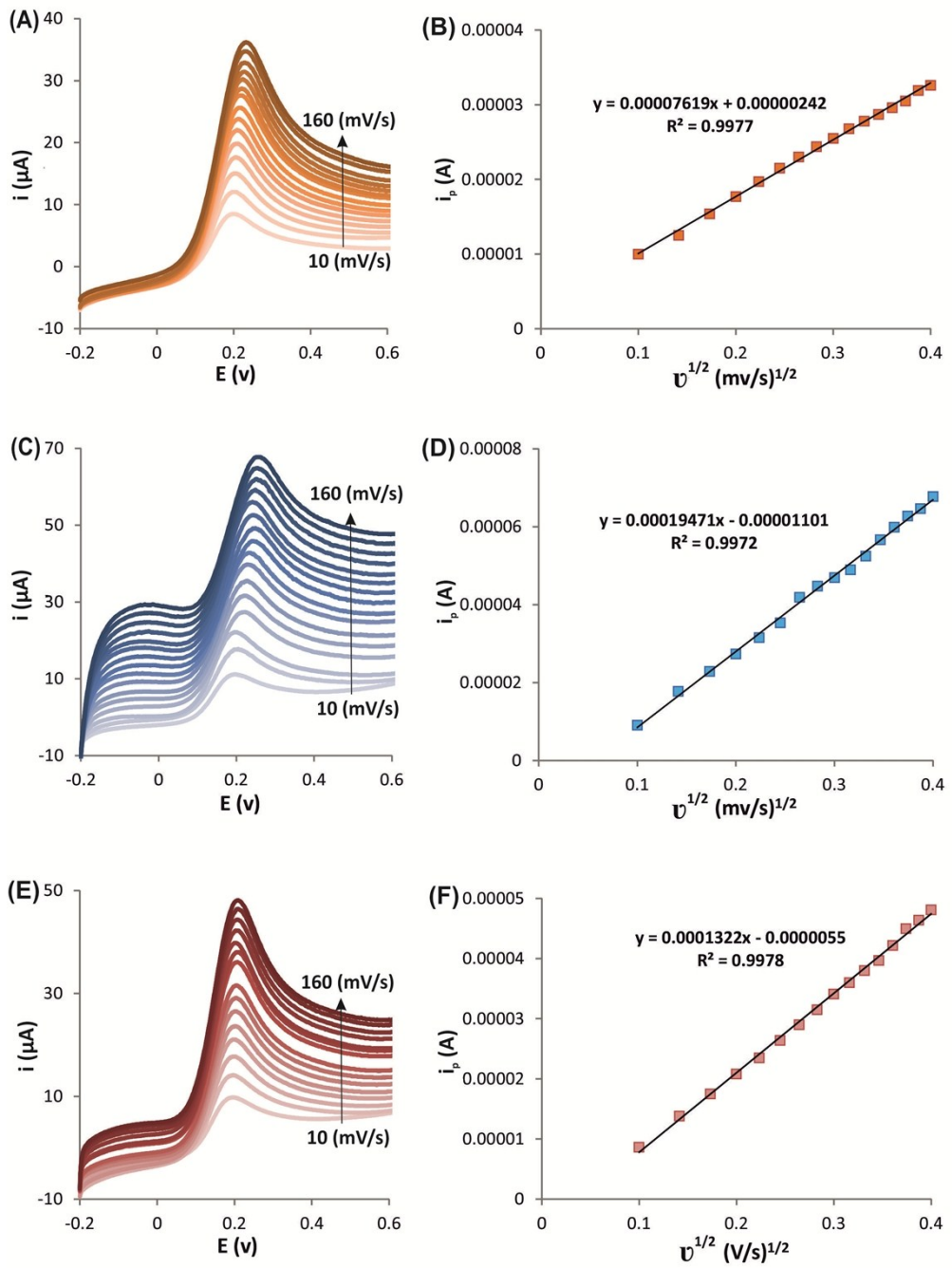


**Fig. S1**. Linear sweep voltammetry (LSV) of 1.0 mM $K_3[Fe(CN)_6]$ and $K_4[Fe(CN)_6]$ in the presence of 0.1 M KCl. Panels A and B represent the LSV and peek current vs. the scan rate square root of the bare AuE, respectively. Panels C and D represent the LSV and peek current vs. the scan rate square root of the MWCNT-AuE, respectively. Panels E and F represent the LSV and peek current vs. the scan rate square root of the Apt-MWCNT-AuE, respectively. Different scan rates (10 - 160 mV $s^{-1}$) were used for the analyses.

## Fluorescent stains

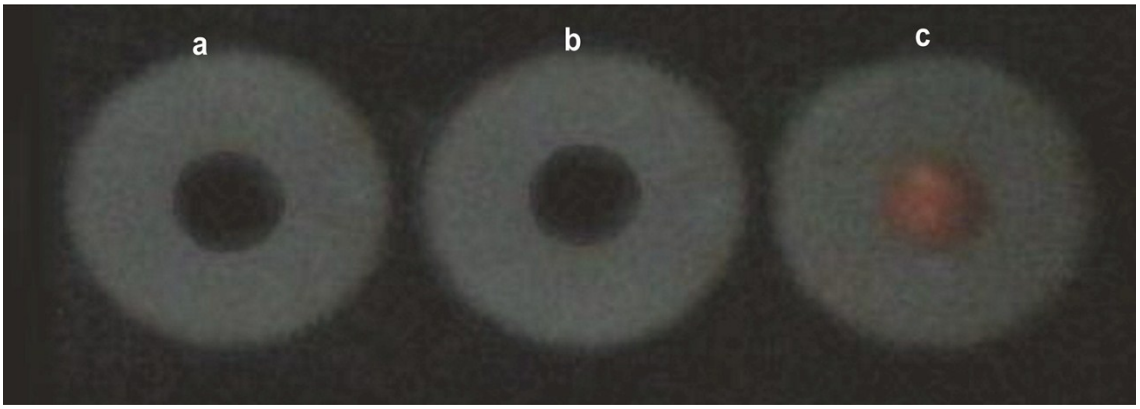


**Fig. S2.** Fluorescent staining of (a) the bare AuE, (b) the MWCNT-AuE and (c) the Apt-MWCNT-AuE after washing steps.

## Optimization

### Effect of pH and supporting electrolyte on the CC-PSA signals of Trp

To find an optimal pH for the development of Trp aptasensor, CC-PSA signals were recorded in a Britton–Robinson (B.R.) buffer (0.1 M) adjusted for pH ranging from 2.0 to 9.0. It was observed that as pH of the supporting electrolyte gradually increased the measured potentials shifted slightly towards less positive values (Fig. S3, panel A). This suggests that the quantity of protons present in the supporting electrolyte determines the amount of Trp absorbed onto the MWCNT layer. We speculated that the maximum values of Trp near the isoelectric point may be due to the nonpolar nature of Trp at this point, and/or increased CC-PSA signals with rise of pH from 2.0 to 7.0 resulting in enhanced surface adsorption of Trp. The maximum value of CC-PSA signals of Trp recorded at pH 7.0. As such a pH of 7.0 was selected as the optimal pH for the rest of this study. Moreover, an equal number of electrons and protons involved in the oxidation of Trp ($\alpha$= 0.5) was calculated from the plot of breakdown/pitting potential ($E_p$) vs pH with the slope of −0.0345 V at the pH range of 2.0-9.0 (Fig. S3, panel A, inset).

The effect of the supporting electrolyte on the CC-PSA results was surveyed using different types of buffers (0.1 M) such as acetate (AC), citrate (CT), B.R. and PBS. Among these buffers, PBS resulted in the best peak in respect to peak shape and intensity (Fig. S3, panel B). Hence, this medium was employed for all analyses performed in this study. Further, ionic strength of the PBS buffer was optimised by the analysis of buffer solutions of different ionic concentrations ranging from 0.005 to 0.14 M. It was found that the lower the concentration of supporting electrolyte is, the more improved the CC-PSA outcome will be. This is explainable as the analyte readily adsorbs onto the electrode surface where biproducts can also be removed easily resulting in the reduction of background signals. Since the best response was recorded at 0.01M PBS, it was selected for further studies (Fig. S3, panel B, inset).

**The effect of the amount of deposited MWCNTs on the CC-PSA signal**

In this study, some common modifiers such as polyaniline, polypyrrole, silver nanoparticles (NPs), non-functionalised MWCNTs, carboxylated MWCNTs, and thiolated-MWCNTs were tested for signal amplification capabilities (data not shown). Application of MWCNTs generally, except for thiolated-MWCNTs, resulted in the best enhancement of signal amplification and the sensitive detection of Trp, in large part due to the unique electrochemical properties of MWCNTs. In fact, both non-functionalised MWCNTs and carboxylated MWCNTs showed similar behavior in terms of the oxidation of Trp. However, the deposition of carboxylated MWCNTs on the Au electrode was more uniform than for the non-functionalised MWCNTs. The CC-PSA signals were significantly enhanced by an increase in the content of carboxylated MWCNTs (up to 12 μg), but reached a saturation above this value (Fig. S3, panel C).

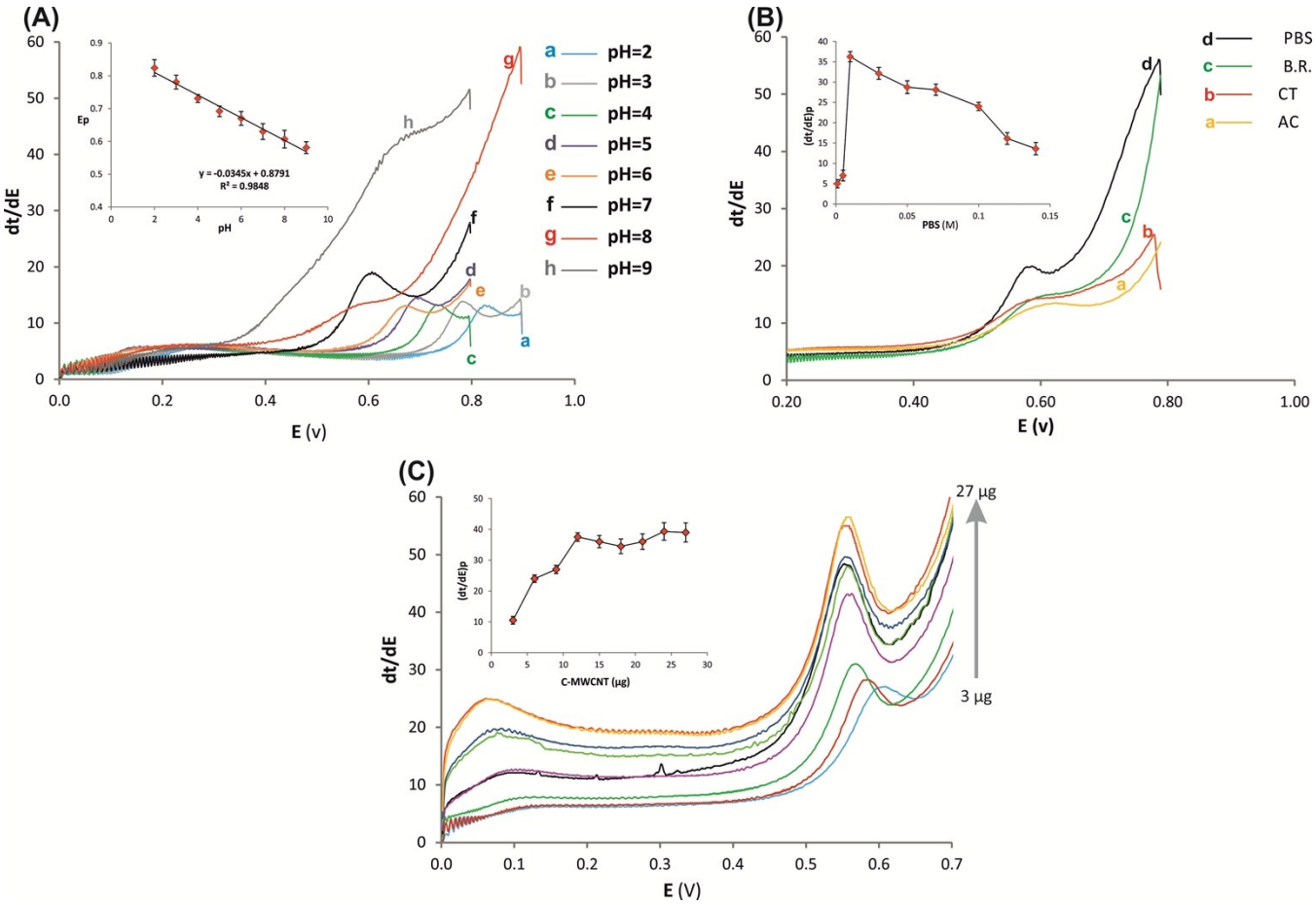


**Fig. S3.** Effects of the pH and the content of deposited MWCNT on CC-PSA of the MWCNT-AuE. A) The effect of pH on the CC-PSA results. Inset A) Correlation between pH and the potential peak of CC-PSA in the presence of Trp (50 µM) in Briton Robinson (B.R.) buffer (0.1 M). B) The effect of the type of buffer on the CC-PSA results. Inset B) The CC-PSA signals obtained using various concentrations of PBS buffer at pH 7. C) The effect of content of the deposited MWCNTs (3, 6, 9, 12, 15, 18, 21, 24, and 27 µg) on the CC-PSA results. Inset C) The plot of the peak values of CC-PSA signals corresponding to the various content of the deposited MWCNT.

**The effect of CC-PSA parameters on the CC-PSA signals of Trp**

Conditional potential ($E_c$), conditioning time ($t_c$) and stripping current ($i_s$) of CC-PSA experiments were optimised in our study. By keeping $i_s$ at +10 μA and $t_c$ at 30 sec, the optimal $E_c$ evaluated in the potential range of 0.0 V to −1.3 V was found to be −0.2 V (Fig. S4, panel A). Applying such a potential in each step of CC-PSA measurement was necessary to initiate renewing and removing the oxidised analytes, or any other impurities from the electrode surface. Beyond -0.2 V, CC-PSA signals are decreased markedly, partly due to the formation of byproducts from oxidation of Trp molecules, therefore −0.2 V was considered as the $E_c$ value for further studies. Furthermore, the effect of applied $t_c$ on the intensity of the cc-PSA signals was studied over a period of 1–30 min (Fig. S4, panel B). It was found that 10 sec is the most favorable period for obtaining a maximum CC-PSA signal that stabilised after 10 sec, indicating that after this time Trp molecules presented in the solution no longer underwent additional interactions with MWCNTs on the electrode surface. Therefore, 10 sec time course was considered as an optimal $t_c$ value of CC-PSA experimentation. With an optimised $E_c$ and $t_c$, we studied is in the range of 3-1000 μA. It should be stated that without applying the potential or current, the oxidation rate of most chemicals is very slow, including Trp. It was therefore critical to employ an external current or potential for fast electrochemical reaction. In this study and optimal $i_s$ was found to be 3 μA in order to achieve maximal recording of CC-PSA signals (Fig. S4, panel C). However, we noted that not only the CC-PSA signal increase with a lowering of $i_s$, but also the background signals appear to increase which add to the detection noise.

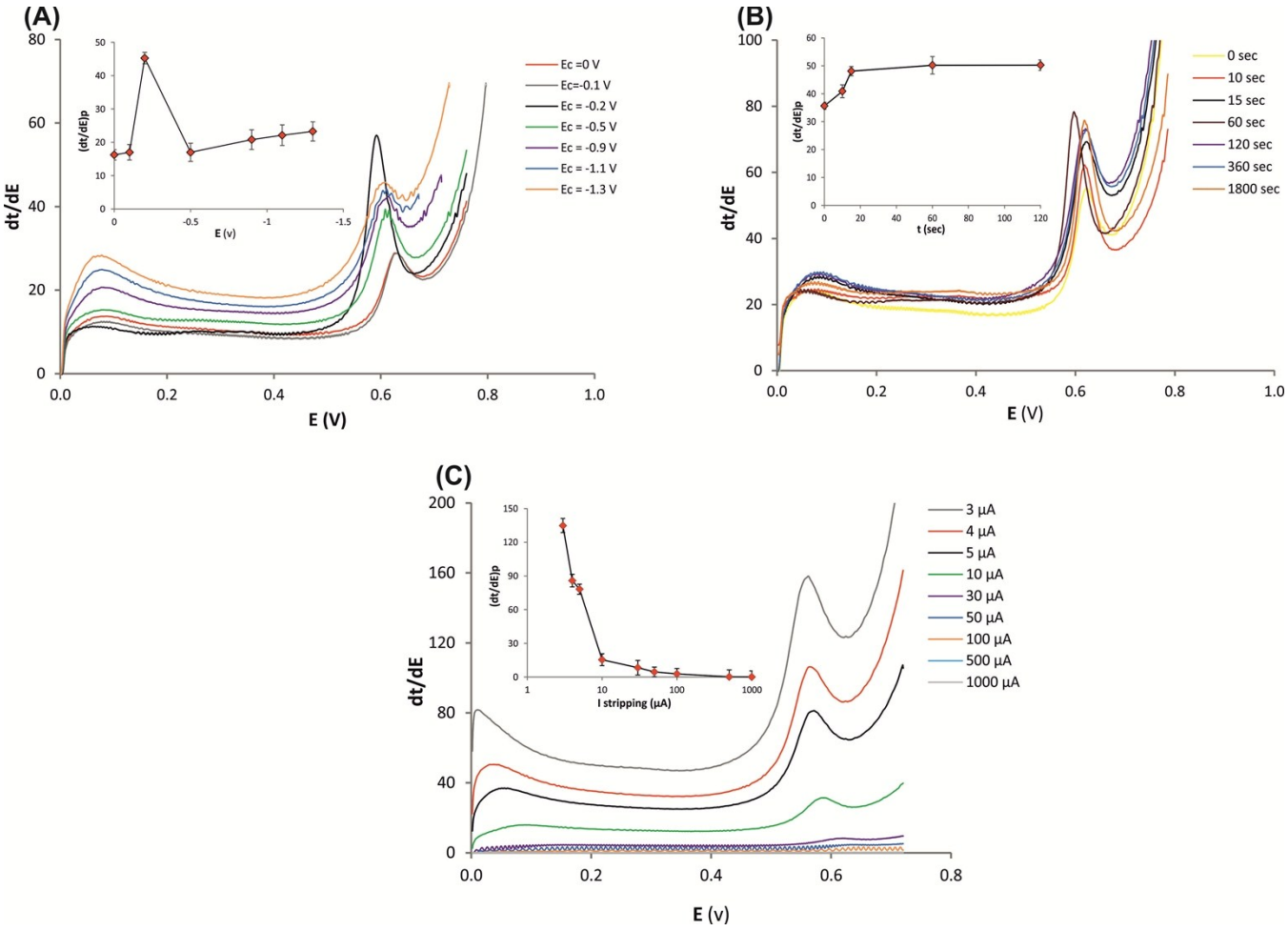


**Fig. S4.** Optimisation of parameters for CC-PSA using MWCNT-AuE. A) Optimisation of the $E_c$ value at $i_s$ = 10 µA and $t_c$ = 30 sec. Inset A) The plot corresponding to the CC-PSA signals for various $E_c$ values. B) Optimisation of the $t_c$ value at $E_c$= -0.2 V and $i_s$= 10 µA. Inset B) The plot corresponding to the CC-PSA signals for various $t_c$ values. C) Optimisation of the $i_s$ value at $E_c$= -0.2 V and $t_c$= 10 sec. Inset C) The plot corresponding to the CC-PSA signals for various $i_s$ values. All these experiments were carried out in the presence of Trp (50 µM).

**Analytical application of the Trp aptasensor**

**Differential pulse voltammetric (DPV) determination of Trp**

Differential pulse voltammetry (DVP) analysis of Trp was performed by scanning the potential ranging from 0.2 to 0.8 V with the following parameters: step potential of 6.0 mV, modulation amplitude of 25.05 mV, modulation time of 0.05 sec and interface time 0.5 sec at the pretreatment step, $E_c$ of −0.2 V applied for 10 sec under stirring (100 rpm). For the calibration of the analytes, DPV from 0.2 to 0.8 V at a scan rate of 12 mV $s^{-1}$ was recorded. The increasing concentration of Trp (from $5.0 \times 10^{-7}$ to $8.0 \times 10^{-5}$) is shown in Fig. S7 (panel A). The plot of $i$ (μA) at $E_p$ vs. concentration was linear in the range of $1.0 \times 10^{-6}$ to $4.0 \times 10^{-5}$ M for Trp (Fig. S5, panel A and B). The LOD (S/N = 3) of $6.0 \times 10^{-7}$ M was obtained, using DPV.

**Chronoamperometric (CA) determination of Trp**

The determination of Trp by MWCNT-AuE was also studied by chronoamperometric (CA). CA determination of Trp were carried out by setting the working electrode potential at 0.9 V vs. $Hg_2Cl_2$/Hg/KCl (3.0 M) for the various concentration of Trp in PBS (pH 7.0). A "one potential-step" technique at potential of 0.9mV vs. $Hg_2Cl_2$/Hg (sat'd) was applied for this purpose. Fig. S5 (panels C and D) shows the amperometric responses for the modified electrode in the absence and presence of Trp over a concentration range of $1.0 \times 10^{-6}$ to $1.3 \times 10^{-4}$ M. The concentration was linear at two ranges of $5.0 \times 10^{-6}$ to $6.0 \times 10^{-5}$ M and $6.0 \times 10^{-5}$ to $1.3 \times 10^{-4}$ M for Trp, and the LOD of $4.9 \times 10^{-6}$ M was obtained using CA.

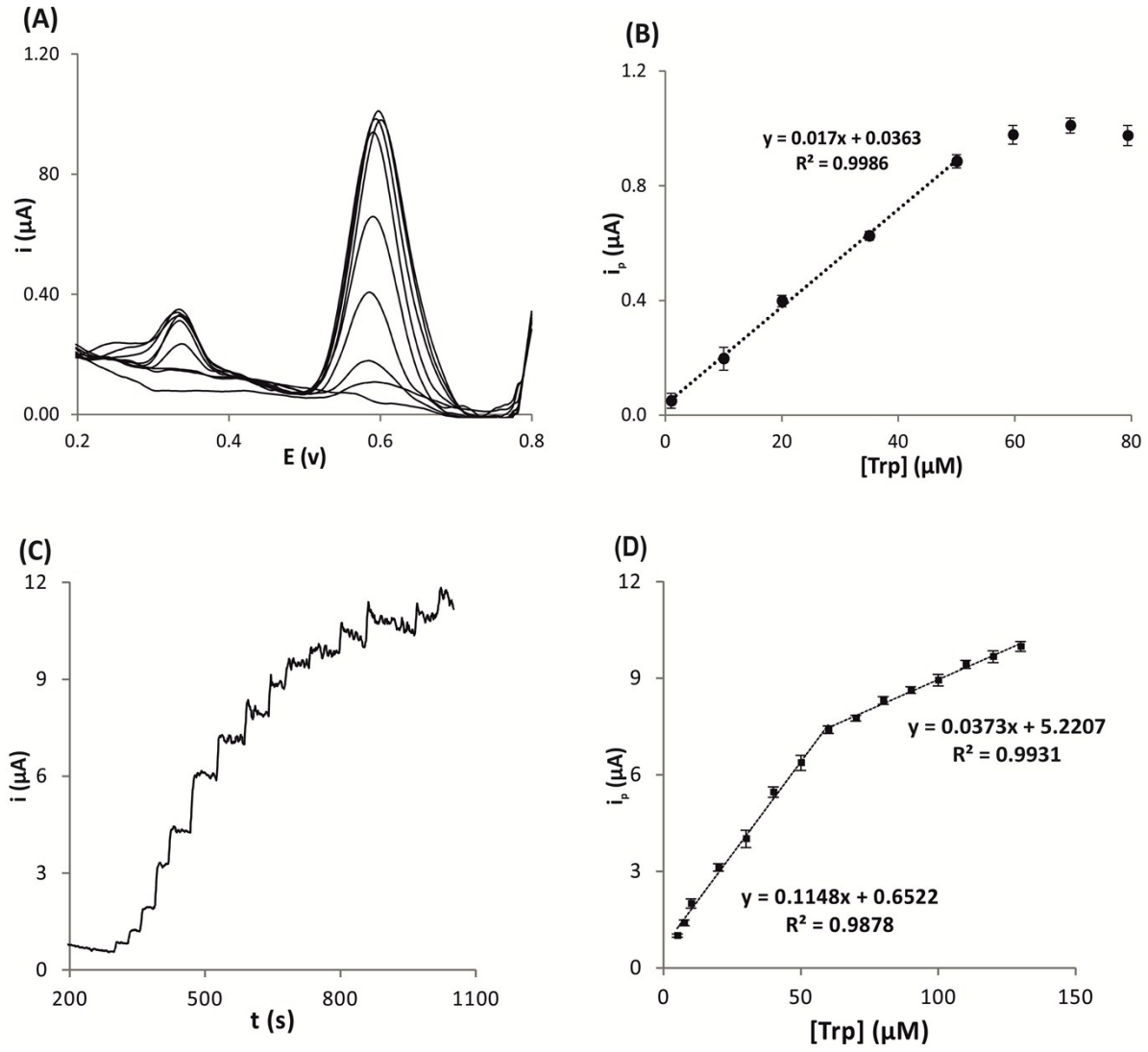


**Fig. S5.** Differential pulse voltammetry (DPV) and chronoamperometry (CA) analyses. A) The baseline-corrected differential pulse voltammograms of Trp analysed using Apt-MWCNT-AuE in 0.01 M PBS (pH=7.0) at the Trp concentration ranging from from $5.0 \times 10^{-7}$ to $8.0 \times 10^{-5}$ at the scan rate of 12.0 mV $s^{-1}$. B) The calibration curve for the Trp determination by DPV. C) The CA for the Apt-MWCNT-AuE in presence of Trp over a concentration range of $1.0 \times 10^{-6}$ to $1.3 \times 10^{-4}$ M at the applied potential of 0.9 V in 0.01 M PBS (pH 7.0; 1000 rpm). D) The calibration curve for the Trp determination by CA.

**Interference study**

Accuracy of the developed sensor dictates the reproducibility of the device. Hence, the concentration of Trp in Aminoven 10 % (1000 ml of Aminoven 10 %contain: Isoleucine 5.00 g, Leucine 7.40 g, Lysine acetate 9.31 g = Lysine 6.60 g, Methionine 4.30 g, Phenylalanine 5.10 g, Threonine 4.40 g, Tryptophan 2.00 g, Valine 6.20 g, Arginine 12.00 g, Histidine 3.00 g, Alanine 14.00 g, Glycine 11.00 g, Proline 11.20 g, Serine 6.50 g, Tyrosine 0.40 g, Taurine 1.00 g) as a commercially available product containing various amino acids was analysed by CV, DPV and CC-PSA (Fig. S6 and Table S1).

**Table S1.** The results of standard addition for Trp analysis in Aminove 10%

| Technic | $V_{PBS}$ (mL) | $V_{Amino}$ (μL) | $[Trp]_{real}$ (g $L^{-1}$) | $[Trp]_{exp}$ (g $L^{-1}$) | R (%) |
|---|---|---|---|---|---|
| CV | 10 | 500 | 0.095 | 0.293 | 307.15 |
| DPV | 10 | 50 | 0.010 | 0.025 | 247.21 |
| CC-PSA | 10 | 100 | 0.020 | 0.020 | 101.62 |

**$[Trp]_{exp}$:** experimental concentration of Trp, **$[Trp]_{real}$:** Real concentration of Trp, **R:** recovery**,** **$V_{Amino}$:** volume of aminoven added, **$V_{PBS}$:** volume of buffer.

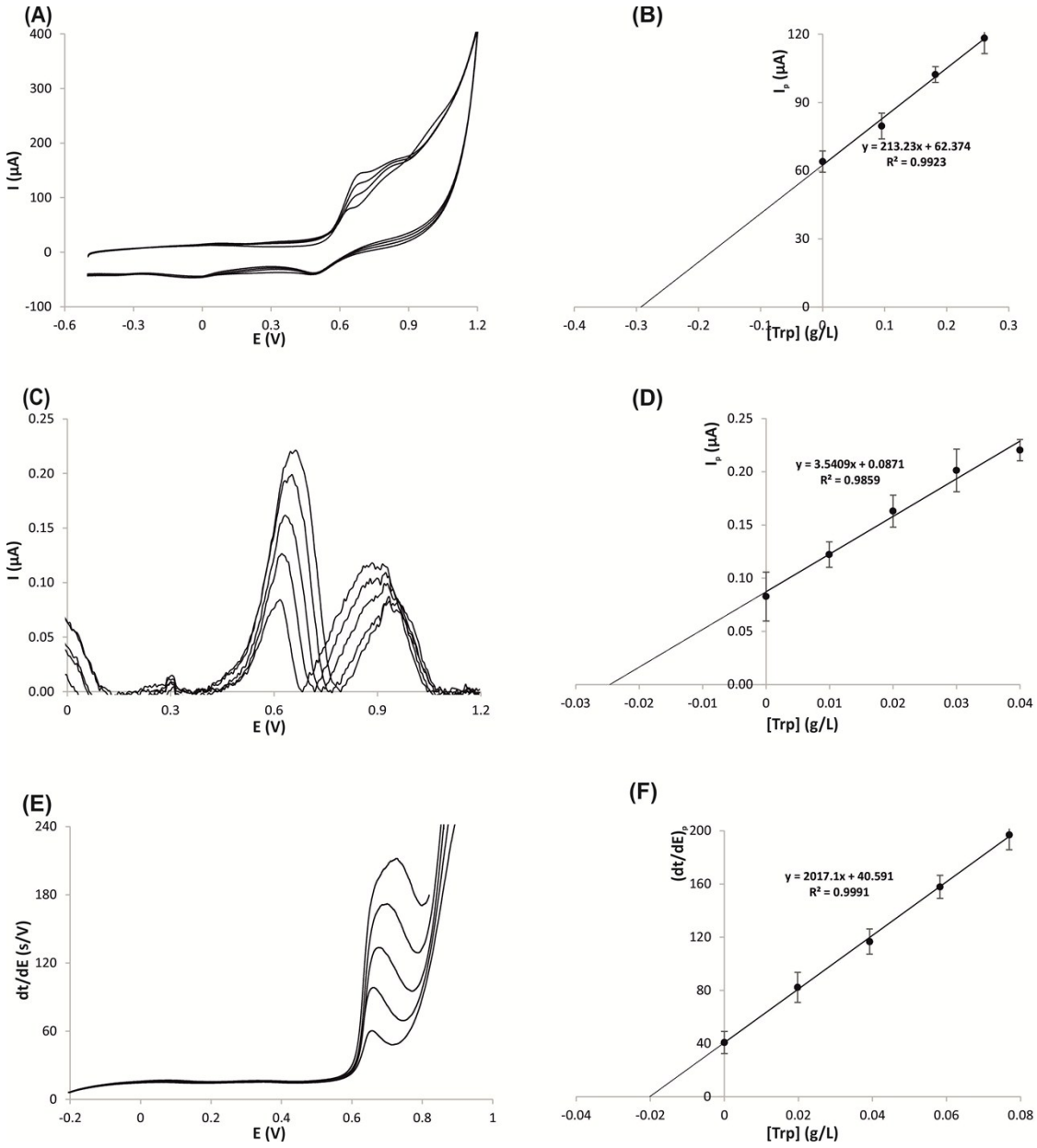


**Fig. S6.** Analyses of Trp content in Aminoven by Apt-MWCNT-AuE. Designated addition of Trp into Aminove 10% was performed for the accuracy of Trp detection. Panels A, C, and E represent the CV, DPV, and CC-PSA analyses, respectively. Panels B, D and F illustrate the calibration curves of the corresponding standard addition.

**Analysis of Trp in real samples**

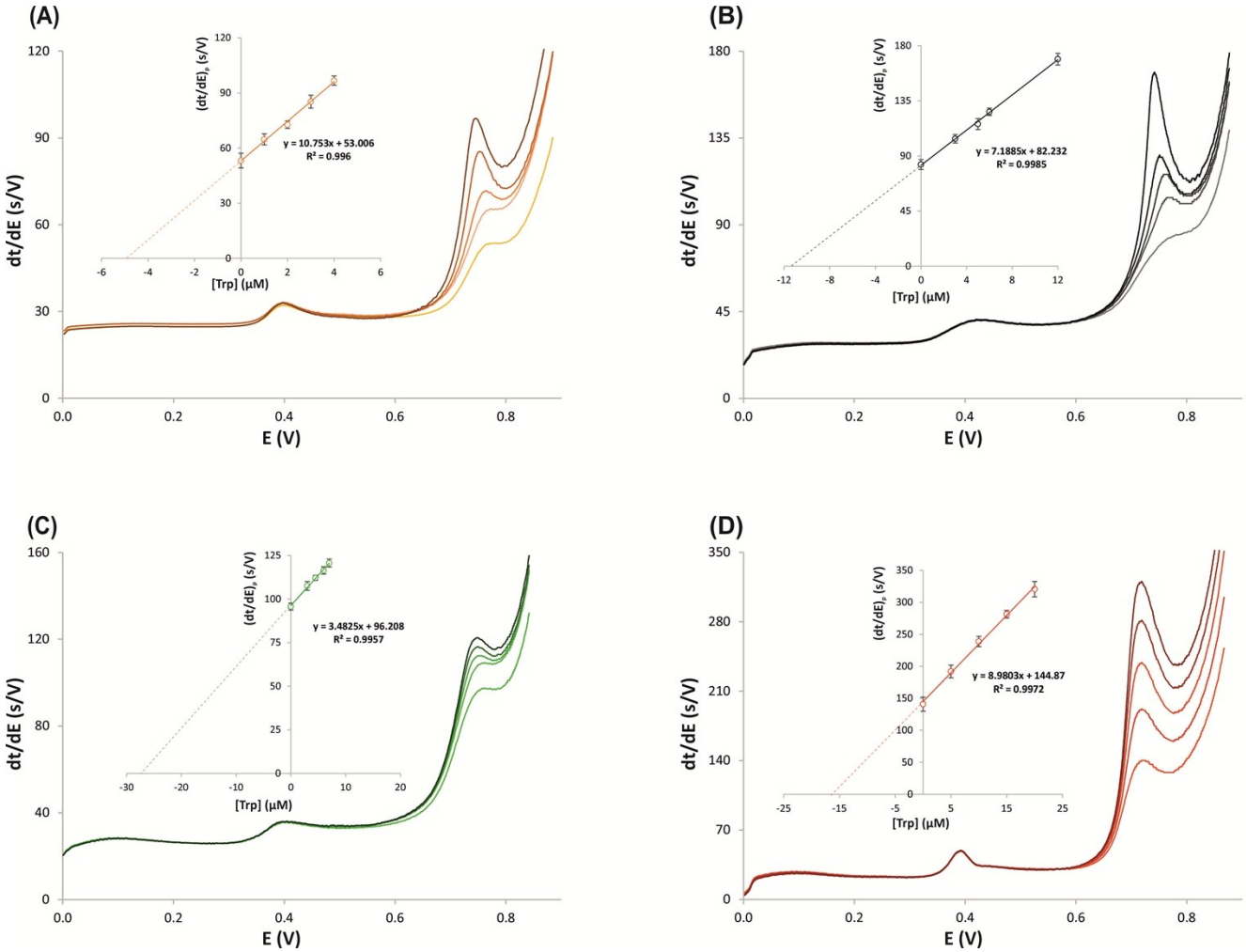


**Fig. S7.** The CC-PSA results of standard addition of Trp into blood serum (A), saliva (B), milk (C), and urine (D) using Apt-MWCNT-AuE. The inset of panels (A), (B), (C), and (D) respectively represent the calibration curves of the corresponding standard addition.

**Reproducibility, stability and regeneration of the aptasensor**

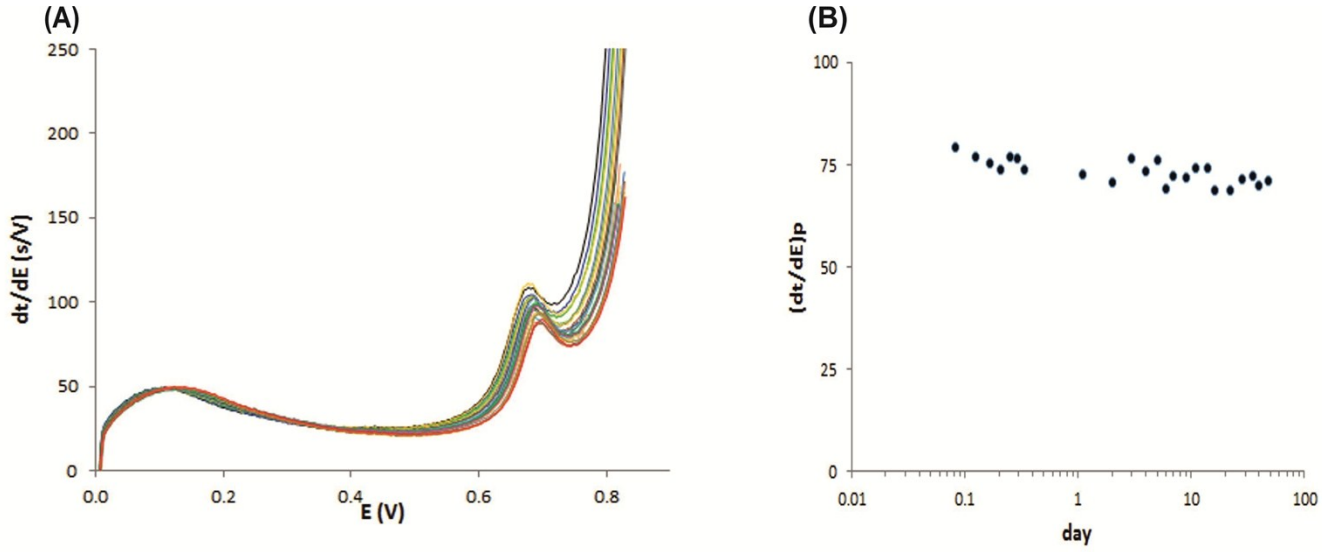


**Fig. S8.** Reproducibility and accuracy assessments of Apt-MWCNT-AuE. A) Reproducibility of CC-PSA results. B) The signals of CC-PSA of Trp (10 μM) performed using within 2-8 hour and 1– 48 day of analysis.

## References

1. Q. Xu and S.-F. Wang, *Microchim. Acta*, 2005, **151**, 47-52.